Journal of the American Heart Association

ORIGINAL RESEARCH

Biomarker Periodic Repolarization Dynamics Indicates Enhanced Risk for Arrhythmias and Sudden Cardiac Death in Myocardial Infarction in Pigs

Julia Bauer; Julia Vlcek, DVM; Valerie Pauly; Nora Hesse; Ruibing Xia; Li Mo, MSc;
Aparna Sharma Chivukula, MSc; Hannes Villgrater; Marie Dressler; Bianca Hildebrand; Eckhard Wolf, DVM;
Konstantinos D. Rizas, MD; Axel Bauer, MD; Stefan Kääb, MD; Philipp Tomsits, MD*;
Dominik Schüttler, MD*; Sebastian Clauss, MD*

BACKGROUND: Periodic repolarization dynamics (PRD) is an electrocardiographic biomarker that captures repolarization instability in the low frequency spectrum and is believed to estimate the sympathetic effect on the ventricular myocardium. High PRD indicates an increased risk for postischemic sudden cardiac death (SCD). However, a direct link between PRD and proarrhythmogenic autonomic remodeling has not yet been shown.

METHODS AND RESULTS: We investigated autonomic remodeling in pigs with myocardial infarction (MI)–related ischemic heart failure induced by balloon occlusion of the left anterior descending artery (n=17) compared with pigs without MI (n=11). Thirty days after MI, pigs demonstrated enhanced sympathetic innervation in the infarct area, border zone, and remote left ventricle paralleled by altered expression of autonomic marker genes/proteins. PRD was enhanced 30 days after MI compared with baseline (pre-MI versus post-MI: 1.75±0.30 deg^2 versus 3.29±0.79 deg^2, $P<0.05$) reflecting pronounced autonomic alterations on the level of the ventricular myocardium. Pigs with MI-related ventricular fibrillation and SCD had significantly higher pre-MI PRD than pigs without tachyarrhythmias, suggesting a potential role for PRD as a predictive biomarker for ischemia-related arrhythmias (no ventricular fibrillation versus ventricular fibrillation: 1.50±0.39 deg^2 versus 3.18±0.53 deg^2 [$P<0.05$]; no SCD versus SCD: 1.67±0.32 deg^2 versus 3.91±0.63 deg^2 [$P<0.01$]).

CONCLUSIONS: We demonstrate that ischemic heart failure leads to significant proarrhythmogenic autonomic remodeling. The concomitant elevation of PRD levels in pigs with ischemic heart failure and pigs with MI-related ventricular fibrillation/SCD suggests PRD as a biomarker for autonomic remodeling and as a potential predictive biomarker for ventricular arrhythmias/survival in the context of MI.

Key Words: autonomic remodeling ■ ischemic heart failure ■ periodic repolarization dynamics ■ pig model ■ sudden cardiac death

Ischemic heart disease affects 154 million patients worldwide.[1,2] Patients with myocardial infarction (MI) are at increased risk for cardiac arrhythmias and sudden cardiac death (SCD).[3] Even though most arrhythmic events occur in the first 48 hours after MI, malignant tachyarrhythmias can appear months later.[4,5] Approximately 30% of all post-MI deaths are due to SCD.[6] In fact, most SCDs occur in the context

CLINICAL PERSPECTIVE

What Is New?

- For the first time, a promising clinical biomarker, periodic repolarization dynamics (PRD), was measured in a preclinical pig model together with an assessment of cardiac autonomic remodeling and the risk for arrhythmias/sudden cardiac death.
- Sympathetic hyperinnervation and altered expression of neural markers resulting in regional differences of sympathetic innervation were accompanied by elevated PRD levels in pigs with ischemic heart failure.
- Elevated baseline PRD identified pigs at increased risk of developing ischemia-induced ventricular fibrillation or sudden cardiac death.

What Are the Clinical Implications?

- We confirm PRD as a marker for autonomic remodeling in a close-to-human porcine model.
- PRD may be a noninvasive predictor of ventricular fibrillation/sudden cardiac death in the context of ischemia and could therefore be a diagnostic tool to optimize preventive strategies in patients at risk.

Nonstandard Abbreviations and Acronyms

BZ	border zone
CTL	control animals without ischemic heart failure
DANISH	Danish Study to Assess the Efficacy of ICDs in Patients With Non-ischemic Systolic Heart Failure on Mortality
EU-CERT-ICD	European Comparative Effectiveness Research to Assess the Use of Primary Prophylactic Implantable Cardioverter-Defibrillators
GAP43	growth associated protein 43
HR	heart rate
HRV	heart rate variability
IHF	ischemic heart failure
LSG	left stellate ganglion
NGF	nerve growth factor
NGFR	nerve growth factor receptor
PRD	periodic repolarization dynamics
SCD	sudden cardiac death
TH	tyrosine hydroxylase
TWA	T-wave alternans

of ischemic heart disease and are mostly driven by ventricular tachyarrhythmias, particularly ventricular fibrillation (VF).[7,8] Proarrhythmic mechanisms include structural, electrical, immunological, and autonomic remodeling processes, which evolve in response to cardiac ischemia.[9–12] The autonomic nervous system is especially closely connected to arrhythmogenesis: sympathetic and parasympathetic innervation modulate electrical activity and conduction with disturbance of this fragile balance facilitating arrhythmias.[13–17] More information about the cardiac autonomic nervous system[14] and its role in VF[18] can be found in 2 excellent review articles by Shen, Rubart, and Zipes.[14,18] Imbalances between the sympathetic and parasympathetic branch with overactivity in catecholaminergic nerves (as has been demonstrated in ischemic heart failure [IHF][19]) are known to facilitate malignant ventricular arrhythmias.[12,17,20,21] Autonomic alteration further fortifies disease maintenance and progression.[12] Both increased sympathetic nerve activity and autonomic remodeling of the cardiac nervous system are associated with arrhythmias. For one, increased activity of the stellate ganglion is seen immediately before the onset of arrhythmias.[22] In addition, sympathetic stimulation in infarcted rabbits has been shown to destabilize ventricular repolarization. This results in locally enhanced transmural dispersion of repolarization in the peri-infarct zone and may serve as a potential proarrhythmic mechanism.[23] On the other hand, repolarization dispersion correlated with increased sympathetic innervation in this model.[23] Moreover, a link between increased nerve density and the occurrence of ventricular arrhythmias was demonstrated in hearts of transplant recipients.[16] Nerve growth factor (NGF) infusion into the left stellate ganglion (LSG) in dogs after MI induced hyperinnervation and resulted in increased vulnerability for VF and SCD, further indicating a proarrhythmic role of autonomic remodeling.[24] Periodic repolarization dynamics (PRD) is a noninvasive ECG-based marker that measures instability of cardiac repolarization in the low frequency spectrum and has been suggested as a biomarker to assess the sympathetic effect on the left ventricular myocardium and inhomogeneity of autonomic signaling.[25] PRD seems to be a promising marker due to strong evidence to predict mortality and SCD in patients with ischemic and nonischemic cardiomyopathy in large clinical studies.[25–29]

However, the specific link between PRD as a high-risk marker and proarrhythmogenic autonomic remodeling

on tissue level has not yet been revealed, because tissue samples from patients are sparse. Likewise, the underlying (patho)physiologic mechanisms of proarrhythmic autonomic remodeling are complex and still not fully understood. To address this, we investigated autonomic remodeling on an immunohistological and molecular level in a preclinical close-to-human pig model of IHF in the context of PRD changes. Our goal was to study autonomic remodeling on different levels and in different regions of the left ventricle (LV; in relation to the ischemia damage) and to experimentally validate PRD as a biomarker for proarrhythmic autonomic remodeling in the heart and to test its potential value as a predictor for SCD in a preclinical pig model.

METHODS

The data that support the findings of this study are available from the corresponding author upon reasonable request.

Animal Model

Three- to 4-month-old German landrace pigs were obtained from *Landwirtschaftliche Forschungsstation Thalhausen*, Technical University of Munich, Kranzberg, Germany; the Center for Innovative Medical Model, Ludwig-Maximilian University (LMU), Oberschleissheim, Germany; and *Lehr- und Versuchsgut der LMU*, Oberschleissheim, Germany. All experiments were approved by Regierung von Oberbayern (ROB-55.2-2631. Vet_02-10-130, ROB-55.2-2532.Vet_02-15-209, and ROB-55.2-2532.Vet_02-18-69) and were conducted in accordance with the *Guide for the Care and Use of Laboratory Animals* at the Institute of Surgical Research at the Walter-Brendel-Centre of Experimental Medicine, Munich, Germany. Seventeen animals with IHF and 11 control animals without IHF (CTL) were included in our analysis. Pigs were randomly assigned to 1 of the 2 groups. Before randomization, pigs were carefully inspected to assess potential exclusion criteria, which were defined a priori (any sign of anatomic malformation, chronic disease, infection, inflammatory disease). Furthermore, pigs were excluded in case of pericardial tamponade, hemorrhagic shock, acute pulmonary edema, severe electrolyte imbalance, apathic behavior, severe pain despite analgetic treatment, fever >41°C despite antibiotic and antiphlogistic treatment, cyanosis, and weight loss >15%. Sample size calculation was performed for the primary end point of PRD 30 days after infarction. A mean±SD value of 1.50±1.0 deg^2 was assumed in CTL, because PRD varies in healthy humans from 1.50 to 3.64 deg^2 among different studies and relatively low PRD values were expected due to anesthesia.[30–33] A minimum increase of 75% was

expected between CTL and pigs with IHF based on the observed PRD in patients with infarction.[27] Applying a 2-sample *t* test, a sample size of 11 pigs per group was estimated to analyze the primary end point. Due to the pigs' mortality in the context of MI, 6 additional pigs were instrumented.

IHF was induced as previously described in detail.[34,35] Briefly, MI was percutaneously induced via balloon occlusion of the left anterior descending coronary artery (LAD) distal to the first diagonal branch for 90 minutes. The LAD was accessed by a standard coronary catheter through a sheath inserted in the right carotid artery. Correct location and balloon occlusion were repeatedly confirmed by angiography. Before induction of MI, high-resolution (1000 Hz) ECGs were recorded in the Frank lead configuration. In addition, levocardiography was performed. Thirty days postinfarction, high-resolution ECG measurements as well as levocardiography were repeated before heart removal for histology and expression analyses. Experiments were performed in total intravenous anesthesia, which was maintained with fentanyl (0.05 mg/kg) and propofol (0.5 mg/kg per min). Tissue from the infarct area, border zone (BZ), and LV (remote to infarct area) was processed separately to further assess autonomic remodeling. Control pigs were treated accordingly without induction of MI.

Ejection Fraction

To measure the left ventricular ejection fraction (EF) and to confirm the IHF phenotype, we performed levocardiography in CTL and pigs with IHF in 2 different angulations (30° left anterior-oblique) and (0° anterior–posterior [AP]) at a paced heart rate (HR) of 130 beats per minute (bpm) using a 6F or 7F pigtail catheter (n=5 CTL and n=7 pigs with IHF).

Periodic Repolarization Dynamics

PRD was measured in the beginning of the intervention using high-resolution ECGs (Schiller medilog AR4 plus 1000 Hz) in the Frank lead configuration (X, Y, and Z leads) in pigs with IHF before and 30 days after MI, as well as in CTL. ECG episodes with a duration of 15 minutes were analyzed. ECGs were manually preprocessed, and artifacts were excluded from analysis. PRD was calculated according to previously published technologies.[25] Briefly, the spatiotemporal information of each T wave was integrated into a single vector T. The instantaneous degree of repolarization instability was assessed by the angle dT° between 2 successive repolarization vectors and plotted over time showing its typical oscillations in the low pseudofrequency range (0.0286–0.1 Hz). PRD was then calculated via continuous wavelet transformation.[25]

Immunofluorescence Staining

After organ harvest, tissue samples were placed in 4% formalin for 24 hours, preserved in 70% ethanol, and then embedded into paraffin. The paraffin blocks were cut into 5-μm thick slices. We performed immunofluorescence staining for tyrosine hydroxylase (TH) and GAP43 (growth associated protein 43). A citrate buffer was used for antigen retrieval. For permeabilization, the tissue was incubated with 0.5% Triton X-100 in PBS for 10 minutes. To reduce autofluorescence TrueBlack (Biotium) was administered for 30 seconds. Blocking was performed with 10% goat serum in 1% BSA in PBS for 90 minutes. The primary antibodies for TH (Abcam, ab112, 1:500 diluted in blocking solution) or GAP43 (GeneTex, GTX30199, 1:500 diluted in blocking solution) were incubated at 4 °C overnight. On the next day, the secondary antibody goat anti-rabbit IgG Alexa Fluor 488 (Cell Signaling, 4412S) diluted 1:500 (TH) or 1:1000 (GAP43) in 1% BSA in PBS was incubated for 1 hour. To visualize the nuclei, sections were stained with Hoechst 33342 (Thermo Fisher Scientific Inc, diluted 1:1000 in PBS) for 10 minutes. Slides were mounted with Dako Fluorescence Mounting Medium (Agilent, S3023). For each sample, at least 2 slides were stained. At least 5 images per slide were taken on an epifluorescence microscope (DM6 B, Leica Microsystems) with a 40× objective. Because pronounced heterogeneity in nerve density after MI has been previously described,[36] we selected areas with the highest nerve density for imaging, as described by other groups.[19,37–40] The number of nerve fibers per field of view was counted using ImageJ software. Immunofluorescence staining was performed in the LVs of 5 control animals and in the LV, BZ, and infarct area of 6 animals with IHF.

Western Blot

Protein lysates were generated from the respective heart regions of 5 animals per group by grinding 100 to 200 mg of frozen tissue with a hammer, dispensing it in Kranias buffer (30 mmol/L Tris pH 8.8, 5 mmol/L EDTA pH 8.0, 30 mmol/L NaF, 3% SDS, 10% glycerol, protease inhibitor [cOmplete Mini, Roche], and phosphatase inhibitor [PhosSTOP, Roche]) and homogenizing it with ultrasound. Protein concentrations were measured using a BCA Protein Assay Kit (Thermo Fisher Scientific). Equal amounts of protein (20, 30, or 40 μg for TH, GAP43, and NGF antibody, respectively) were loaded into a 12% polyacrylamide gel. After gel electrophoresis proteins were transferred to a nitrocellulose membrane, blocked with ROTI block (Carl Roth) for 1 hour and incubated with the primary antibodies TH (1:500, Abcam, ab112), GAP43 (1:10.000, GeneTex, GTX30199), or NGF (1:500, Abbexa, abx173738) overnight at 4 °C. After washing with TBST-0.1%, membranes

Table. Primer Pairs Used for RT-qPCR

Gene	Primer sequence
NGF	F: GGGCCCAATAACGGCTTTTC R: ACATTACGCTATGCACCTCAGT
NGFR	F: TACATCGCCTTCAAGAGGTGGA R: GTCCACAGAGATGCCACTGTC
GAPDH	F: TCGGAGTGAACGGATTTG R: CCTGGAAGATGGTGATGG

F indicates forward primer; R, reverse primer; GAPDH, glyceraldehyde-3-phosphate dehydrogenase; NGF, nerve growth factor; NGFR, nerve growth factor receptor; and RT-qPCR, quantitative real-time polymerase chain reaction.

were incubated with horseradish peroxidase–conjugated secondary antibodies (Abcam, ab97051, 1:5000 or ab131368, 1:2000) for 90 minutes. Proteins were visualized with ECL Western blotting substrate (Thermo Fisher Scientific). After stripping, the above-described protocol was repeated with GAPDH (1:30.000, Abcam, ab190304) for normalization. The integrated density of bands was determined using ImageJ software.

Quantitative Real-Time Polymerase Chain Reaction

Total RNA was extracted from 7 animals per group (from the same cardiac regions as described above) using a mirVana miRNA Isolation Kit (Thermo Fisher Scientific). The manufacturer's protocol was followed after 100 mg of tissue was grinded with a hammer: 500 ng total RNA was reversely transcribed with SuperScript IV Reverse Transcriptase (Thermo Fisher Scientific). We used Sybr Green to perform quantitative real-time polymerase chain reaction. Primer pairs were designed with Primer-BLAST (National Institutes of Health) (Table) or purchased by a commercial vendor (GAP43: qSscCED0009710, BioRad). The primer specificity was confirmed by melting curve analysis and gel electrophoresis. GAPDH was used as a housekeeping gene. All samples were amplified in duplicates. Relative gene expression was quantified using the ΔCt-method. For TH, no working primer pair could be designed.

Statistical Analysis

Data are presented as mean±SEM. GraphPad Prism 8 (GraphPad Software) was used for statistical analysis. Shapiro–Wilk-test was used to check for normality. Differences between the 2 groups were calculated by unpaired Student *t* test or Mann–Whitney test accordingly. PRD levels between 2 different time points in the same group were compared by paired Student *t* test or Wilcoxon test, respectively. To compare the incidence of VF and SCD between the groups, Fisher exact test was used. A *P* value <0.05 was considered statistically significant. Data of immunofluorescence, Western blot,

and polymerase chain reaction were normalized to the respective control. Infarct areas, BZs, and LVs of the IHF group were compared with LVs of the control group.

RESULTS

Reduced EF After MI

The IHF phenotype was confirmed by angiography 30 days after MI, demonstrating markedly reduced left ventricular EF in IHF pigs compared with CTL (0° anterior–posterior, EF, CTL versus IHF: 61.08±2.58% versus 27.39±4.06%, $P<0.001$ [Figure 1A]; 30° left anterior-oblique, EF, CTL versus IHF: 56.74±2.08% versus 32.16±4.94%, $P<0.01$ [Figure 1B]).

Increase in Sympathetic Nerve Fiber Density After MI

To assess autonomic remodeling, we investigated sympathetic nerve density. Here, immunofluorescence staining revealed a significant increase in TH-positive nerve fiber density in IHF pigs compared with CTL (Figure 2). This increased nerve density of TH-positive nerve fibers was seen in the remote LV, BZ, and infarct area (CTL LV versus IHF LV: 1.00±0.13 versus 1.65±0.10, $P<0.01$ [Figure 2A, 2B, and 2E]; CTL LV versus IHF BZ: 1.00±0.13 versus 2.27±0.21, $P<0.001$ [Figure 2A, 2C, and 2E]; CTL LV versus IHF infarct area: 1.00±0.13 versus 2.22±0.31, $P<0.01$, [Figure 2A, 2D, and 2E]). GAP43 was used as a marker for sprouting nerve fibers.[41,42] The density of GAP43-positive sprouting nerve fibers was significantly higher in the remote

LV, BZ, and infarct area in the IHF group compared with the LV in the control group (CTL LV versus IHF LV: 1.00±0.05 versus 1.50±0.08, $P<0.001$ [Figure 3A, 3B, and 3E]; CTL LV versus IHF BZ: 1.00±0.05 versus 1.60±0.06, $P<0.001$ [Figure 3A, 3C, and 3E]; CTL LV versus IHF infarct area: 1.00±0.05 versus 1.49±0.19, $P<0.05$ [Figure 3A, 3D, and 3E]).

Regional Upregulation of Neural Proteins After MI

Western blot analyses (Figure 4) showed no alteration in TH protein expression in the remote LV compared with control levels (CTL LV versus IHF LV: 1.00±0.05 versus 1.16±0.07, $P=0.09$) (Figure 4A). The BZ showed a trend towards an increased TH protein expression without reaching statistical significance (CTL LV versus IHF BZ: 1.00±0.04 versus 1.66±0.31, $P=0.06$) (Figure 4A). TH protein expression was significantly elevated in the infarct area (CTL LV versus IHF infarct area: 1.00±0.08 versus 4.10±0.68, $P<0.01$) (Figure 4A). GAP43 protein expression was similar to TH protein expression with no change in the remote LV (CTL LV versus IHF LV: 1.00±0.02 versus 1.00±0.02, $P=0.93$) (Figure 4B), a nonsignificant trend in BZ (CTL LV versus IHF BZ: 1.00±0.10 versus 1.99±0.44, $P=0.06$) (Figure 4B), and a significantly higher expression in the infarct area (CTL LV versus IHF infarct area: 1.00±0.11 versus 1.56±0.20, $P<0.05$) (Figure 4B) compared with control LV. In addition, we found unchanged NGF protein levels in remote LV (CTL LV versus IHF LV: 1.00±0.11 versus 1.03±0.04, $P=0.81$) (Figure 4C), but the increase in NGF protein
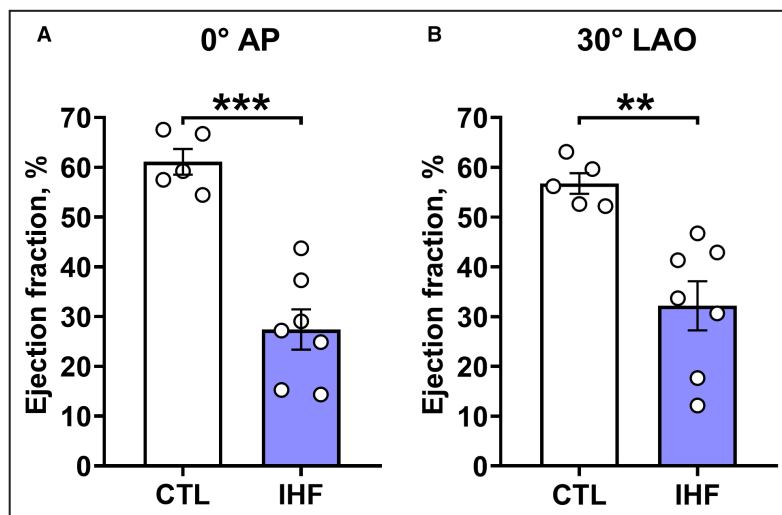

Figure 1. Ejection fraction (EF).
A, EF of control animals without ischemic heart failure (CTL) and animals with ischemic heart failure (IHF) assessed by levocardiography in 0° anterior–posterior (AP) angulation. **B**, EF of CTL and animals with IHF assessed by levocardiography in 30° left anterior-oblique (LAO) angulation. Bar graphs represent mean±SEM and circles represent data of individual pigs. Unpaired t test. **$P<0.01$; ***$P<0.001$.
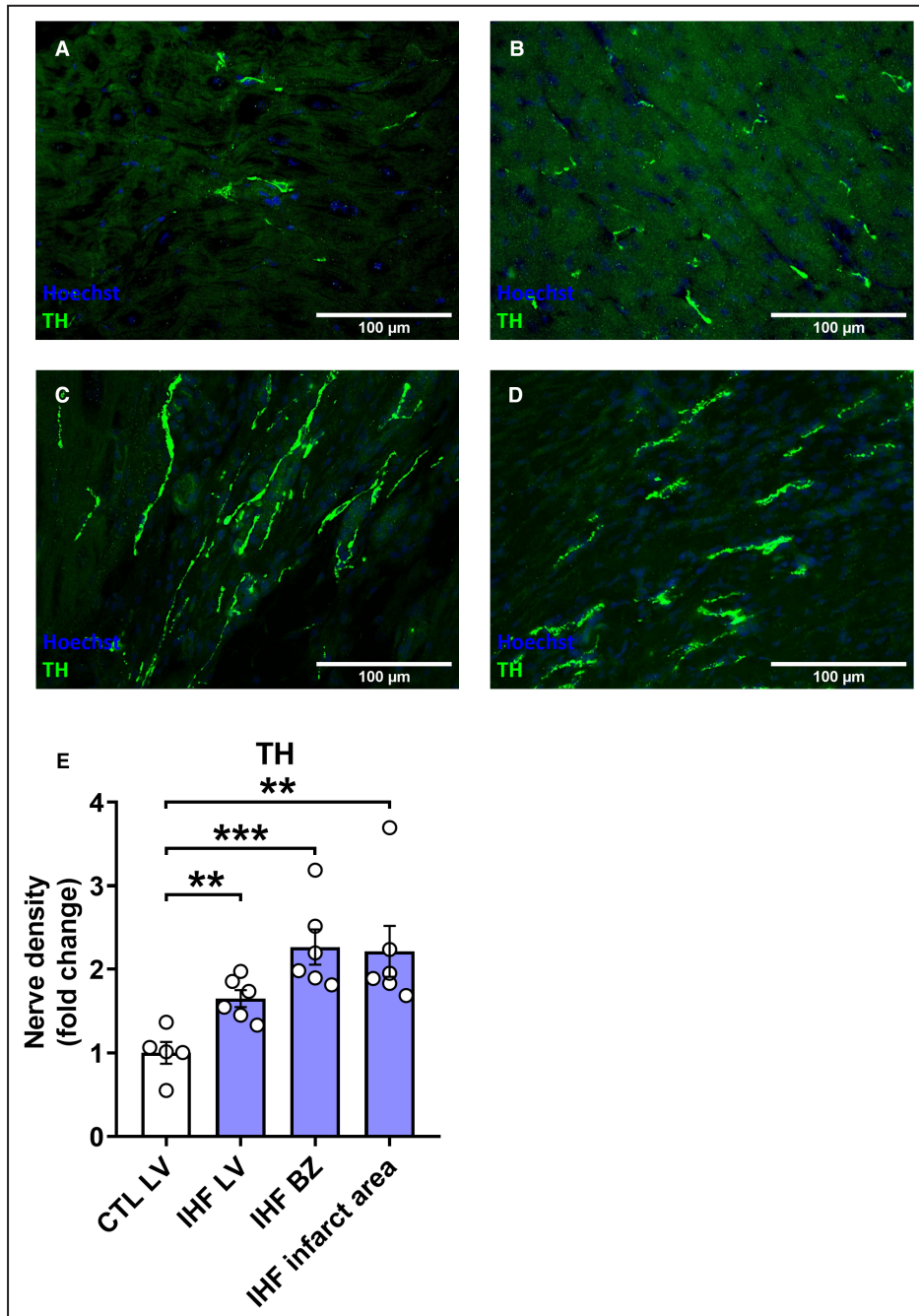
Figure 2. Sympathetic nerve density assessed by tyrosine hydroxylase (TH) immunofluorescence staining.

A–D, Representative TH immunofluorescence images of the left ventricle (LV) of control animals without ischemic heart failure (CTL) (**A**), the LV of animals with ischemic heart failure (IHF) (**B**), the border zone (BZ) of animals with IHF (**C**), and the infarct area of animals with IHF (**D**). TH-positive nerve fibers are shown in green and nuclei in blue. **E,** TH+ nerve density (fold change compared with LV in control pigs). Bar graphs represent mean±SEM and circles represent data of individual pigs. Unpaired *t* test and Mann–Whitney test. *$P<0.05$; **$P<0.01$; ***$P<0.001$.

expression reached significance in the BZ and infarct area (CTL LV versus IHF BZ: 1.00±0.16 versus 2.10±0.39, $P<0.05$; CTL LV versus IHF infarct area: 1.00±0.07 versus 3.69±0.43, $P<0.001$) (Figure 4C).

Dysregulation of Neural Gene Expression After MI

We studied gene expression (Figure 5) of GAP43, NGF, and NGF receptor (NGFR). GAP43 was downregulated
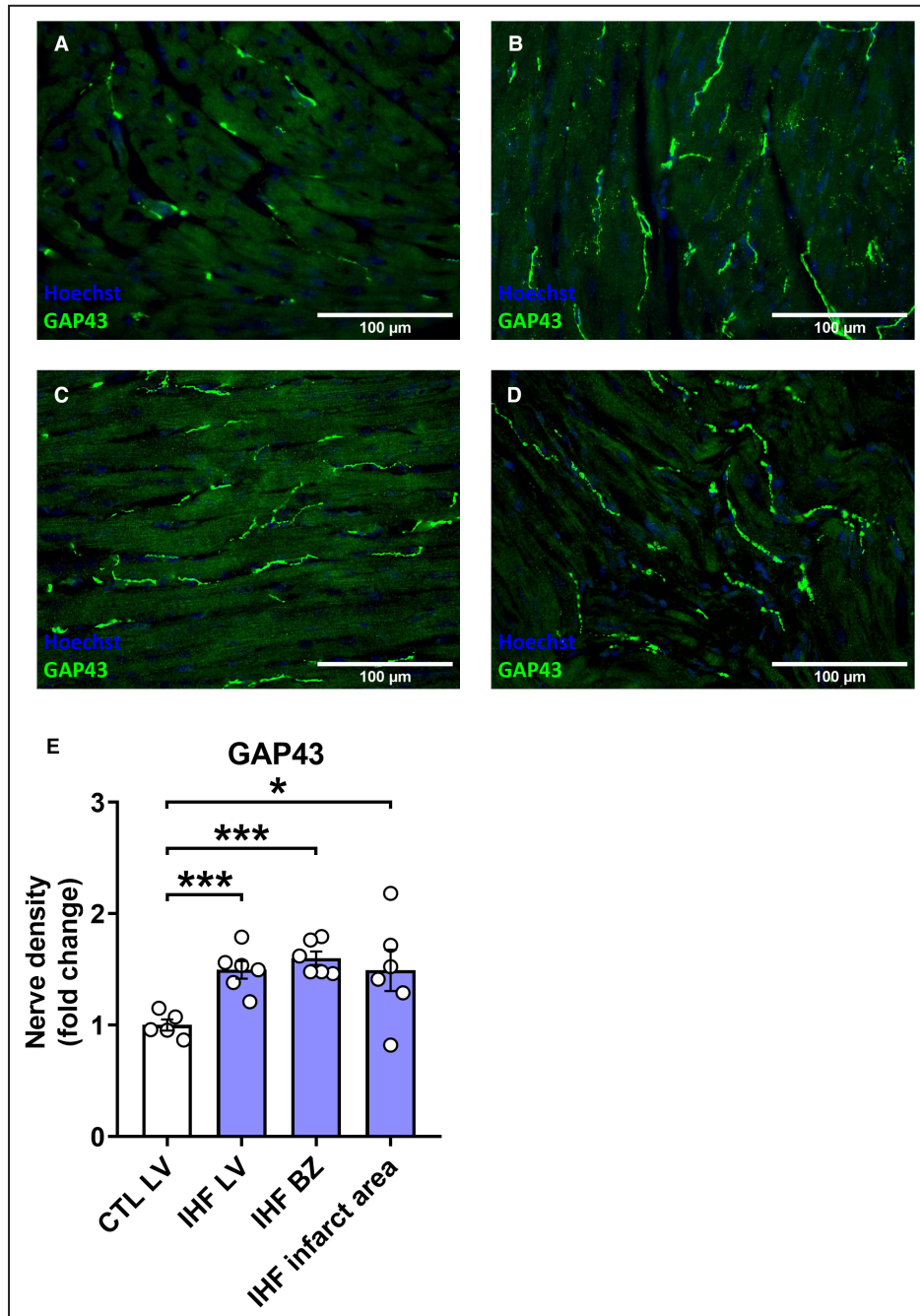
Figure 3.   Sprouting nerve density assessed by GAP43 (growth associated protein 43) immunofluorescence staining.

A–D, Representative GAP43 immunofluoresecence images of the left ventricle (LV) of control animals without ischemic heart failure (CTL) (A), the LV of animals with ischemic heart failure (IHF) (B), the border zone (BZ) of animals with IHF (C), and the infarct area of animals with IHF (D). GAP43-positive nerve fibers are shown in green and nuclei in blue. E, GAP43+ nerve density (fold change compared with LV in control pigs). Bar graphs represent mean±SEM and circles represent data of individual pigs. Unpaired t test. *$P<0.05$; **$P<0.01$; ***$P<0.001$.

in the remote LV after MI compared with control animals (GAP43 CTL LV versus IHF LV: 1.00±0.31 versus 0.11±0.04, $P<0.05$ [Figure 5A]). In the BZ GAP43, messenger RNA was unchanged and in the infarct area GAP43 expression was increased nonsignificantly compared with the LV in control pigs (GAP43 CTL LV versus IHF BZ: 1.00±0.31 versus 0.94±0.36, $P=0.90$; GAP43 CTL LV versus IHF infarct area: 1.00±0.31 versus 2.90±1.29, $P=0.16$ [Figure 5A]). NGF gene expression remained unchanged in the remote LV and
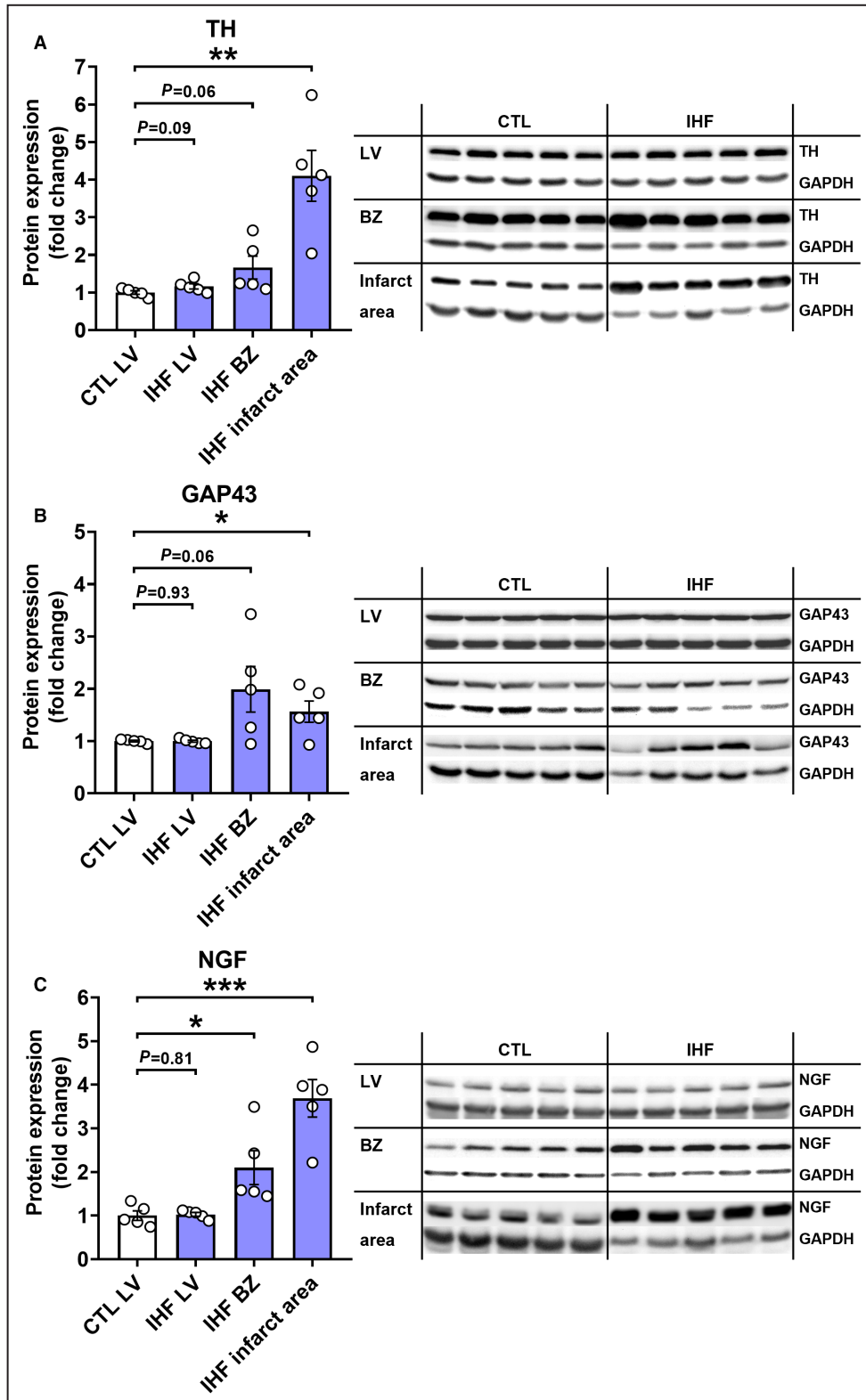
Figure 4. Protein expression of tyrosine hydroxylase (TH), growth associated protein 43 (GAP43), and nerve growth factor (NGF).
A–C, Protein expression (fold change compared with the left ventricle [LV] in control pigs) of TH (**A**), GAP43 (**B**), and NGF (**C**) with respective representative Western blot images of TH (**A**), GAP43 (**B**), NGF (**C**), and corresponding GAPDH images. BZ indicates border zone; CTL, control animals without ischemic heart failure; and IHF, animals with ischemic heart failure. Bar graphs represent mean±SEM and circles represent data of individual pigs. Unpaired t test. *$P<0.05$; **$P<0.01$; ***$P<0.001$.
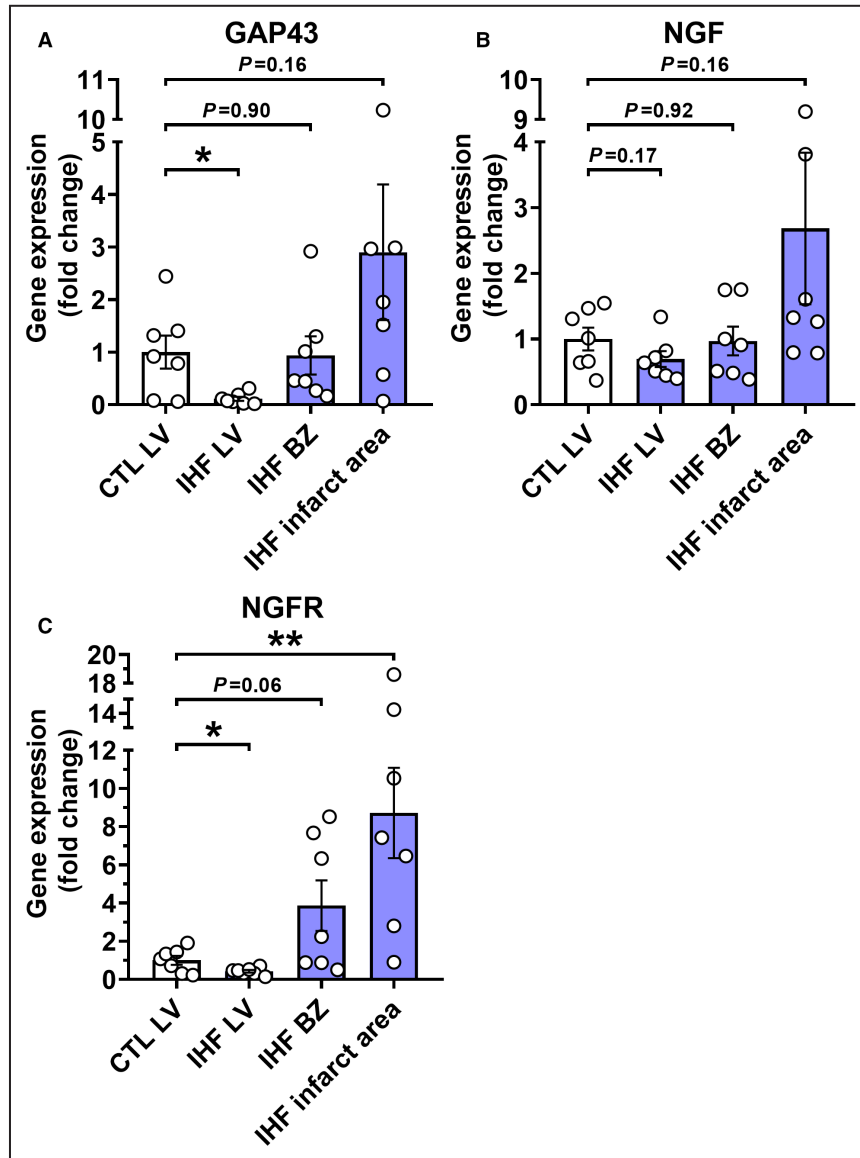
Figure 5.   Gene expression of GAP43 (growth associated protein 43), nerve growth factor (NGF), and NGF receptor (NGFR).
A–C, Gene expression (fold change compared with the left ventricle [LV] in CTL pigs) of GAP43 **(A)**, NGF **(B)**, and NGFR **(C)**. Bar graphs represent mean±SEM, circles represent data of individual pigs. BZ indicates border zone; CTL, control animals without ischemic heart failure; IHF, animals with ischemic heart failure. Unpaired *t* test and Mann–Whitney test. *P<0.05; **P<0.01.

in the BZ (NGF CTL LV versus IHF LV: 1.00±0.17 versus 0.69±0.12, P=0.17; NGF CTL LV versus IHF BZ: 1.00±0.17 versus 0.97±0.22, P=0.92 [Figure 5B]). In the infarct area, a trend was seen towards an increase of NGF messenger RNA compared with the LV of control animals (NGF CTL LV versus IHF infarct area: 1.00±0.17 versus 2.68±1.15, P=0.16 [Figure 5B]). NGFR transcript abundance was decreased after MI in the remote LV and showed a trend towards upregulation in the BZ (NGFR CTL LV versus IHF LV: 1.00±0.23 versus 0.42±0.07, P<0.05; NGFR CTL LV versus IHF

BZ: 1.00±0.23 versus 3.86±1.33, P=0.06 [Figure 5C]). In the infarct area, NGFR messenger RNA expression was significantly elevated, showing an almost 9-fold increase compared with the LV of control animals (NGFR CTL LV versus IHF infarct area: 1.00±0.23 versus 8.71±2.36, P<0.01 [Figure 5C]).

Increase in PRD After MI

PRD in the IHF group 30 days after MI was significantly higher than PRD in the control group (CTL versus IHF: 1.52±0.31 deg^2 versus 3.29±0.79 deg^2, P<0.05,
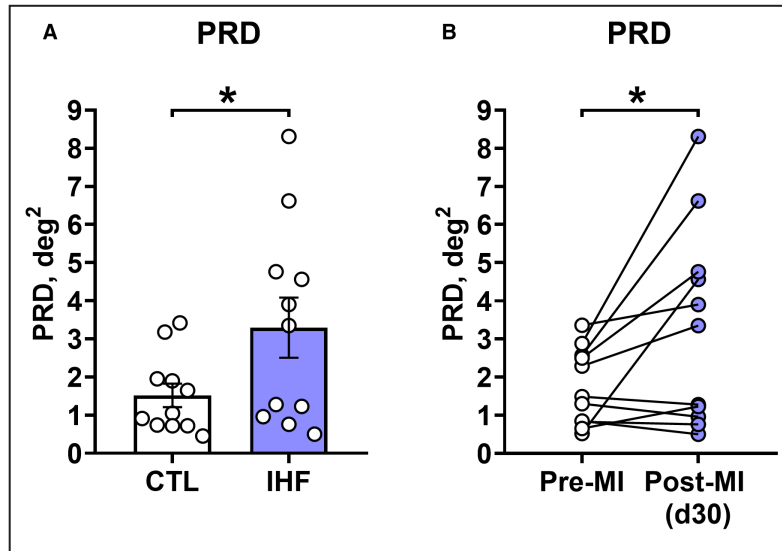
Figure 6. Periodic repolarization dynamics (PRD) levels.
A, PRD levels in control animals without ischemic heart failure (CTL) and animals with ischemic heart failure (IHF). Unpaired *t* test. *$P<0.05$. **B**, Individual PRD levels before and 30 days after myocardial infarction (MI). Paired *t* test. *$P<0.05$. Bar graphs represent mean±SEM and circles represent data of individual pigs.

unpaired *t* test [Figure 6A]). Likewise, individual PRD was significantly elevated 30 days after MI compared with baseline PRD before MI (pre-MI versus post-MI: 1.75 ± 0.30 deg^2 versus 3.29 ± 0.79 deg^2, mean of differences 1.55 ± 0.63, $P<0.05$, paired *t* test [Figure 6B]). Figure S1 shows the dT° signal for a pig before and 30 days after MI.

In the immunofluorescence staining, 3 pigs with high PRD increase and 3 pigs with similar PRD when comparing pre-MI PRD and PRD 30 days post-MI were included. Thus, the selection of animals used for immunostaining was balanced in terms of post-MI PRD increase. When analyzing the 6 pigs used for immunostaining separately, PRD increased by a mean of 158% or 1.60 deg^2 (pre-MI versus post-MI: 1.43 ± 0.36 deg^2 versus 3.03 ± 1.07 deg^2, Wilcoxon test $P=0.44$).

Unchanged HR and HR Variability After MI

HR did not differ significantly between the control and IHF groups (CTL versus IHF: 87.73 ± 5.62 bpm versus 96.64 ± 4.65 bpm; $P=0.24$, unpaired *t* test). The post-MI PRD values of animals with post-MI HR in the lowest and highest quartiles were not significantly different (PRD low HR versus PRD high HR: 4.15 ± 1.56 versus 2.83 ± 0.81; $P=0.49$, unpaired *t* test). However, mean PRD was slightly lower in pigs with higher HRs. HRV parameters were assessed as described in Data S1. The HRV time-domain parameters SD of NN interval duration, square root of the mean of the sum of the squares of differences between adjacent NN intervals,

percent of NN interval differences >50 ms, and SEM, as well as the frequency-domain parameters were unaltered in pigs with IHF compared with control pigs (Table S1).

Pre-MI PRD as a Marker for Elevated Risk of VF and SCD in the Context of MI

Eleven of 17 pigs that underwent MI developed VF (65%) (Figure 7A) and 7 of 17 died of SCD due to refractory VF (41%) (Figure 7C). VF and SCD occurred during LAD occlusion or shortly after the experiment except for 1 pig, that died due to VF during the second experiment 30 days after MI. In contrast, none of the control pigs showed VF. Correspondingly, the occurrence of VF and SCD was significantly higher in the IHF group compared with the control group (VF CTL versus IHF: 0/11 versus 11/17, $P<0.001$, Fisher exact test [Figure 7A]; SCD CTL versus IHF: 0/11 versus 7/17, $P<0.05$, Fisher exact test [Figure 7C]). To further evaluate PRD as a biomarker indicating an increased risk for arrhythmogenesis in MI, we analyzed baseline PRD in IHF pigs with/without VF or SCD separately. Pigs with MI-related VF showed a significantly elevated PRD pre-MI compared with pigs that did not develop VF (no VF [n=6] versus VF [n=11]: 1.50 ± 0.39 deg^2 versus 3.18 ± 0.53 deg^2, $P<0.05$ [Figure 7B]). Furthermore, in pigs that died due to SCD significantly elevated pre-MI PRD levels were observed compared with pigs that survived MI (no SCD [n=10] versus SCD [n=7]: 1.67 ± 0.32 deg^2 versus 3.91 ± 0.63 deg^2, $P<0.01$ [Figure 7D]).
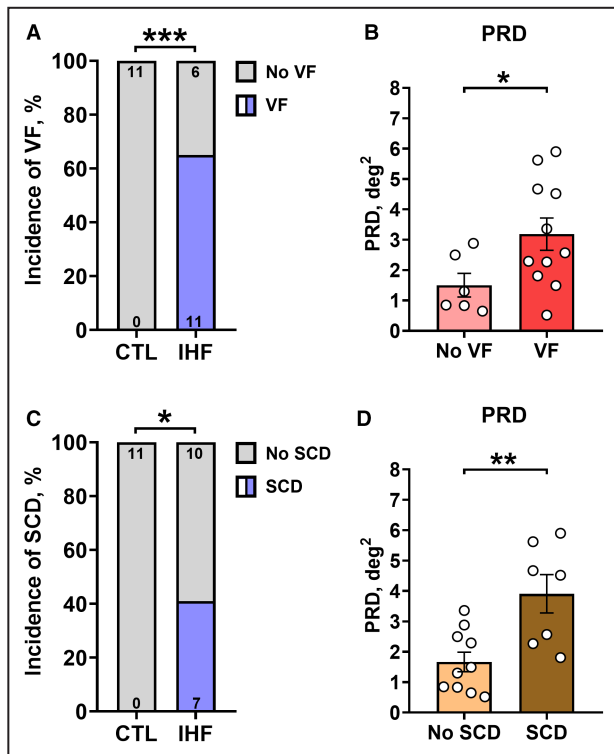
Figure 7. Periodic repolarization dynamics (PRD) levels and susceptibility for ventricular fibrillation (VF) and sudden cardiac death (SCD).

A, Incidence of VF due to myocardial infarction (MI). **B**, PRD levels before MI for pigs depending on VF development due to MI. **C**, Incidence of SCD due to MI. **D**, PRD levels before MI for pigs depending on SCD development due to MI. **A+C**, Numbers in bars represent number of pigs in each group. Fisher exact test. **B+D**, Bar graphs represent mean±SEM and circles represent data of individual pigs. Unpaired *t* test. CTL indicates control animals without ischemic heart failure; and IHF, animals with ischemic heart failure. *P<0.05; **P<0.01; ***P<0.001.

DISCUSSION

In the present study, we aimed to validate PRD as a marker for autonomic remodeling and to investigate its potential value as a biomarker for arrhythmia risk in a preclinical pig model of acute MI-induced IHF.

We used a porcine ischemia–reperfusion model due to various reasons. First, PRD was primarily established as a high-risk marker for mortality and SCD in patients following infarction.[25,26] Second, ischemic heart disease is the most common underlying cause of SCD (≈75% of all SCD cases).[7,43] Third, autonomic remodeling is known to occur in IHF facilitating arrhythmogenesis.[21] Fourth, PRD has already been demonstrated to be assessable in pigs.[25] Fifth, porcine models closely resemble the pathophysiology in humans due to similarities in cardiovascular anatomy and electrophysiology, which makes pigs suitable to study arrhythmogenesis.[44,45] There are only some minor differences in the conduction system compared with

humans, including more densely innervated atrioventricular node, shorter His bundle and Purkinje fibers reaching into transmural myocardium (whereas ending subendocardial in humans) leading to fast electrical coupling, higher HR, and increased excitability under stress.[44,46–48] Thus, our translational approach provides a unique opportunity to preclinically explore the value of a noninvasive biomarker in predicting arrhythmias and SCD and to broaden our knowledge on autonomic remodeling processes. IHF was successfully induced, as seen by the significantly reduced EF compared with control pigs. This is in line with previous studies using ischemia–reperfusion models[34,49] and sets basis for further research on underlying remodeling processes. On gene, protein, and tissue levels, we demonstrated pronounced changes resulting in increased regional dispersion of autonomic innervation in IHF pigs. The observed changes in TH- and GAP43-positive nerve fibers highly suggest a sympathetic hyperinnervation in the whole LV. TH is commonly used to stain sympathetic nerve fibers due to its involvement in the production of catecholamine neurotransmitters.[50] GAP43 is used as a marker for nerve sprouting and branching, as it is expressed especially in neurites and growth cones of developing and regenerating axons.[41,42]

In parts, the literature is still discordant. Whereas mainly hyperinnervation patterns were found after MI, a few studies have shown denervation patterns.[19,36,51–57] Our model clearly demonstrated a heterogenous hyperinnervation as underlined by both in vivo and molecular biology methods. This is in line with various canine studies showing enhanced sympathetic innervation after MI.[19,36] In an MI pig model, increased sympathetic nerve density was observed in the BZ with no change in the remote LV.[54] Rabbits have also shown increased nerve density 7 days after MI in the BZ and remote LV.[55] However, other animal models demonstrated (an additional) denervation. For example, in rats, nerve density was decreased in the infarct area and the LV apex supplied by the LAD distal to the ligation, but also an increased TH expression in areas proximal to the ligation has been observed.[51] Moreover, innervation changes seem to be time dependent as demonstrated by scintigraphy studies in dogs that showed an initial apical denervation and a full reinnervation 14 weeks after MI.[52] In patients with MI, no reinnervation was seen up to 3 months after infarction[53] but could partially be detected between 3 and 12 months after MI.[57]

Interestingly, our immunofluorescence results showed a clear increase in nerve density for TH- and GAP43-positive nerves in IHF animals not only in the infarct area but also in the BZ as well as in the remote LV. This finding is supported by previous studies showing that sympathetic hyperinnervation after MI is not limited to the infarct area. In a dog model, MI leads to an increase of neural markers in the infarct area,

remote LV, and LSG.[19] Even in both atria, sympathetic nerve sprouting was seen in a canine model after MI.[36] A rat model demonstrated regional changes in sympathetic neurotransmission concomitant to the observed changes in general cardiac nerve density with increased sympathetic markers in stellate ganglia and heart areas proximal to the LAD ligation.[51] A forensic case-control study found that patient hearts with old MI had significantly higher sympathetic innervation especially in the BZ than hearts used as controls from patients who died of other reasons, highlighting the relationship between nerve sprouting and SCD after MI.[56]

The mechanisms leading to autonomic changes are still under investigation: Zhou et al showed that retrograde transport of NGF and GAP43 from the infarct area to the LSG and consecutive increased LSG innervation may trigger nerve sprouting in remote areas by increased LSG activity.[19] NGF might be the key player in directing sympathetic hyperinnervation. This neurotrophin is known to positively regulate the growth of neurites from sympathetic neurons[58] and to stabilize GAP43 messenger RNA and thus decelerate its degradation.[59] Transgenic mice overexpressing NGF in the heart showed cardiac hyperinnervation.[60] Chen et al showed that NGF infusion to the LSG leads to sympathetic hyperinnervation and subsequently to higher frequency of ventricular arrhythmias.[61] However, the increased NGF in the BZ can also have beneficial effects. NGF silencing by injection of NGF small interfering RNA in rats with MI showed decreases in NGF, TH, and GAP43 expression in the LV and BZ concomitant with decreased vascular endothelial growth factor and arteriolar and capillary densities in the BZ. This leads to an increased infarction area and lower EF in the NGF-suppressed group compared with MI alone.[62] The enhanced NGF levels we detected might be a possible explanation for sympathetic hyperinnervation as it might function as a possible trigger stimulating formation of new sympathetic fibers.

Expression of neural markers in Western blot and gene expression analyses differed between compartments. Western blots showed the highest increase of neural protein expression in the infarct area, less increased levels in the BZ, and levels comparable with controls in the remote LV of IHF pigs. The expression of genes associated with nerve growth were upregulated in the infarct area, although without reaching significance except for NGFR, probably due to comparably high interindividual deviation. GAP43 and NGFR gene expression was downregulated in the remote LV. We speculate that this might be a sign of a counterregulation to a possible previous upregulation. Thus, remodeling signaling in the remote LV might already be advanced or further proceeded, as seen by sympathetic hyperinnervation. Supporting our results, a peak in expression of

neural markers was seen at 1 week after MI in a canine model.[19] We chose the time point of 30 days after MI to investigate the long-term consequences of autonomic remodeling. In addition, the risk of SCD is 10-fold higher in the first month after survived acute MI than afterwards (1.2% in the first month compared with ≈1.2% per subsequent year[6]). Patients with reduced EF are at an increased risk for SCD of 2.3% in the first month.[63] Clearly, additional studies investigating innervation behavior over the course of time after MI might be interesting. In addition, in contrast to the healthy myocardium in the remote LV, which might show decreased gene expression as a reaction to the existing sympathetic hyperinnervation, the injured myocardium in the infarct area may not be able to react adequately to the present increase of nerve density. The discrepancy between immunofluorescence and Western blotting in the remote left heart could be the result of inhomogeneous nerve distribution that we noticed under the microscope. Because we considered only areas with the highest nerve density and excluded areas of denervation, our staining represents local innervation patterns, whereas our Western blots represent global protein expression. We chose this approach because pronounced heterogeneity in nerve density after MI has been previously described[16,36] and for better comparability with results obtained by others.[19,37–40]

The rate of VF and SCD in the context of MI (65% and 41%, respectively), mostly during or within minutes after acute MI (acute LAD occlusion), was comparatively high in our pig cohort. Calculations of out-of-hospital-mortality for patients with acute MI vary between 9% and 35%,[64–66] adding to the 1.2% risk of SCD in the first month and each following year after survived MI.[6] The fact that VF and SCD occurred around LAD occlusion in IHF pigs and in none of the control pigs (especially not during the invasive diagnostic catheter examination) suggested ischemia as the key trigger of VF in our model.

To evaluate autonomic remodeling noninvasively, we measured PRD, an ECG marker, which assesses instability of cardiac repolarization in the low frequency spectrum. PRD is associated with sympathetic activity and dispersion of sympathetic activity on the level of the ventricular myocardium.

The relationship between sympathetic activity and oscillations in the low frequency spectrum of HRV has been recognized for several decades.[67,68] For instance, physiologic sympathetic activation increases the low frequency spectrum of variability in muscle sympathetic nerve discharges, HR, and systolic arterial pressure.[69] Subsequent to HRV analysis, periodic changes in repolarization indicating repolarization variability and instability were investigated as this phase of the cardiac cycle is highly modulated by sympathetic activity. There are different techniques that allow quantification

of repolarization variability. T-wave alternans (TWA) is an early introduced method analyzing changes in T-wave amplitude between following beats in an ABAB pattern.[70] A canine model of coronary occlusion detected a possible relationship of TWA and sympathetic activity, because TWA decreased after sympathetic denervation and showed that it was temporally associated with the onset of VF in this study, indicating its potential role in predicting arrhythmias.[71] Increased inducibility of ventricular arrhythmias and a reduced rate of arrhythmia-free survival in patients with high TWA support this assumption.[72] Later T-wave oscillations in different frequency spectrums than the TWA were investigated. In patients, mainly with ischemic heart disease, TWA, and T-wave oscillations in 2 different frequency spectrums were increased before the onset of ventricular arrhythmias.[73] The predictive value of TWA is limited among others due to its interdependence to HR and HRV.[70,74] None of these markers have been included in the guidelines to assess the arrhythmia risk in patients after MI. Instead, risk prediction for ventricular arrhythmias and implantable cardioverter-defibrillator recommendation is based on EF in current guidelines.[75,76]

Owing to the important role of the autonomic nervous system in arrhythmogenesis and SCD, there are several therapeutic options that target the autonomic nervous system to prevent ventricular arrhythmias and SCD. In addition to a pharmacologic β-blockade, invasive sympathetic cardiac denervation including left or bilateral stellectomy and stellate ganglion block can prevent further ventricular arrhythmias, though it is a last resort due to its invasiveness and is thus scarcely performed.[77–79]

We found a significant increase of PRD levels 30 days after MI, which parallels the elevation of sympathetic nerve density and the nonuniformly changes of neural protein and gene expression in the remote LV, BZ, and infarct area. Therefore, PRD might not only indicate increased sympathetic activity on a ventricular level but also sympathetic hyperinnervation and remodeling. PRD has been previously described to be fairly independent of HR and HRV.[25,80] PRD and HR rise concordantly during low-intensity training, but PRD does not change when HR is altered by atrial pacing, indicating that PRD can be affected by sympathetic activity but not by HR alone.[80] We investigated HR and HRV parameters, representing autonomic modulation of the sinus node, but found no significant alteration 30 days after MI (Table S1). After MI, PRD values of animals with HRs in the highest quartile were not significantly different from those with HRs in the lowest quartile. The even slightly lower PRD in pigs with higher HRs indicates that the observed PRD increase after MI is not dependent on an increase in HR, but is rather independent of HR.

There is substantial clinical evidence that an increased PRD is a strong and independent marker of cardiac mortality and SCD in patients after infarction as well as in patients with ischemic and nonischemic cardiomyopathy.[25–29] In addition, the prospective EU-CERT-ICD (European Comparative Effectiveness Research to Assess the Use of Primary Prophylactic Implantable Cardioverter-Defibrillators) study and a post hoc analysis of DANISH (Danish Study to Assess the Efficacy of ICDs in Patients With Non-ischemic Systolic Heart Failure on Mortality) found an association between PRD and the treatment effect of ICD implantation in reducing mortality, suggesting that PRD may be a valuable tool for personalized preventive treatment decisions.[28,29] Because in our pigs most arrhythmias and SCDs occurred during or within minutes after acute MI, we studied PRD pre-MI, which is nearly impossible in humans. Interestingly, we found that PRD measured before MI was significantly associated with an enhanced risk for arrhythmias and SCD. Animals that developed VF or died of SCD in the context of MI had significantly higher pre-MI PRD levels. These results suggest a potential role for PRD as a predictive biomarker indicating the risk for arrhythmias/SCD in otherwise healthy pigs with initial MI. From a clinical perspective, assessing PRD in patients with an increased risk for but no history of MI could be a promising approach to identify patients at risk of SCD and thus may then allow optimized primary prevention strategies.

However, conclusions must be drawn with caution, as it is a small experimental animal study. Further validation in large human cohorts is warranted to confirm PRD as a predictive biomarker identifying patients at risk for arrhythmias/SCD.

LIMITATIONS

The focus of this study was to investigate the relationship of autonomic remodeling and PRD. Therefore, other proarrhythmogenic remodeling processes such as electrical and structural remodeling and how they might affect PRD were not investigated. However, the fact that PRD pre-MI and PRD in the CTL group varied widely, although all pigs showed similar EF (data for IHF pigs pre-MI are not shown and data for CTL pigs are shown in Figure 1), indicates that LV function does not majorly affect PRD. Further information about structural and electrical remodeling in IHF pigs are presented in previous work of our group.[34] Anesthesia might have attenuated sympathetic activity and thus might influence PRD values because propofol is known to affect autonomic regulation and lower sympathetic activity.[33,81] Therefore, the overall level of PRD was relatively low. However, all pigs were treated equally with 0.5 mg/kg propofol per minute. Furthermore, we focused

specifically on the sympathetic branch of the autonomic nervous system, because PRD is assumed to be a marker for sympathetic activity on the ventricular level.[25] To get a full picture of the autonomic influence on the heart, parasympathetic alterations should be considered in future studies as well. Another limitation of this study is that it is not possible to strictly discriminate between the influence of intrinsic cardiac autonomic remodeling and the overall sympathetic activity on PRD. In addition to sympathetic hyperinnervation, the sympathetic tone might be increased by the cardiac sympathetic afferent reflex (CSAR) in our model. Humoral factors from the ischemic myocardium can activate sympathetic afferent nerve fibers, which pass the information on to central sites. In addition, mechanoreceptors stimulated by distension might activate sympathetic afferent fibers. Subsequently, the efferent sympathetic tone is increased, which might help to sustain cardiac output in the short term.[12,82] Thus, in the future, additional recordings of stellate ganglion activity might be of interest. Alternatively, assessment of skin nerve activity can give information about stellate ganglion activity and efferent sympathetic tone.[83] However, it seems that not the efferent cardiac tone but rather autonomic remodeling is responsible for PRD differences between groups, because HRV parameters were unchanged after MI. Moreover, we have previously shown that there are no differences in IHF pigs compared with controls in regard to atrioventricular conduction (measured by atrioventricular Wenckebach cycle length and atrioventricular effective refractory period), which would have been affected by cardiac sympathetic afferent reflex.[34]

CONCLUSION

In this study, we demonstrated that IHF leads to pronounced sympathetic hyperinnervation and changes in expression of neural markers. Altered sympathetic innervation patterns result in increased dispersion of autonomic innervation and are paralleled by significantly elevated PRD levels, which suggests PRD as a biomarker for autonomic remodeling. Furthermore, pigs with MI-related VF and SCD show significantly elevated PRD levels even before MI, suggesting PRD as a potential predictive biomarker for ventricular arrhythmias and survival in the context of MI.

ARTICLE INFORMATION

Affiliations

Department of Medicine I, University Hospital, LMU Munich, Munich, Germany (J.B., J.V., V.P., N.H., R.X., L.M., A.S.C., H.V., M.D., B.H., K.D.R., S.K., P.T., D.S., S.C.); German Center for Cardiovascular Research (DZHK), Partner Site Munich, Munich Heart Alliance, Munich, Germany (J.B., V.P., N.H., R.X., L.M., A.S.C., H.V., M.D., K.D.R., A.B., S.K., P.T., D.S., S.C.); Institute of Surgical Research at the Walter-Brendel-Centre of Experimental Medicine, University Hospital, LMU Munich, Munich, Germany (J.B., J.V., V.P., N.H., R.X., L.M., A.S.C., H.V., M.D., P.T., D.S., S.C.); Chair for Molecular Animal Breeding and Biotechnology, Gene Center and Department of Veterinary Sciences, LMU Munich, Munich, Germany (E.W.); Interfaculty Center for Endocrine and Cardiovascular Disease Network Modelling and Clinical Transfer (ICONLMU), LMU Munich, Munich, Germany (E.W., S.K., S.C.); and University Hospital for Internal Medicine III, Medical University of Innsbruck, Innsbruck, Austria (A.B.).

Sources of Funding

Disclosures

None.

Supplemental Material

Data S1

REFERENCES

1. Bauersachs R, Zeymer U, Brière JB, Marre C, Bowrin K, Huelsebeck M. Burden of coronary artery disease and peripheral artery disease: a literature review. *Cardiovasc Ther*. 2019;2019:8295054. doi: 10.1155/2019/8295054

2. GBD 2016 Disease and Injury Incidence and Prevalence Collaborators. Global, regional, and national incidence, prevalence, and years lived with disability for 328 diseases and injuries for 195 countries, 1990-2016: a systematic analysis for the global burden of disease study 2016. *Lancet*. 2017;390:1211–1259. doi: 10.1016/s0140-6736(17)32154-2

3. Huikuri HV, Castellanos A, Myerburg RJ. Sudden death due to cardiac arrhythmias. *N Engl J Med*. 2001;345:1473–1482. doi: 10.1056/NEJMra000650

4. Auffret V, Bourenane H, Sharobeem S, Leurent G, Didier R, Gilard M, Nicol PP, Payot L, Filippi E, Hacot JP, et al. Early and late ventricular arrhythmias complicating ST-segment elevation myocardial infarction. *Arch Cardiovasc Dis*. 2022;115:4–16. doi: 10.1016/j.acvd.2021.10.012

5. Bloch Thomsen PE, Jons C, Raatikainen MJ, Moerch Joergensen R, Hartikainen J, Virtanen V, Boland J, Anttonen O, Gang UJ, Hoest N, et al. Long-term recording of cardiac arrhythmias with an implantable cardiac monitor in patients with reduced ejection fraction after acute myocardial infarction: the cardiac arrhythmias and risk stratification after acute myocardial infarction (CARISMA) study. *Circulation*. 2010;122:1258–1264. doi: 10.1161/circulationaha.109.902148

6. Adabag AS, Therneau TM, Gersh BJ, Weston SA, Roger VL. Sudden death after myocardial infarction. *JAMA*. 2008;300:2022–2029. doi: 10.1001/jama.2008.553

7. Hayashi M, Shimizu W, Albert CM. The spectrum of epidemiology underlying sudden cardiac death. *Circ Res*. 2015;116:1887–1906. doi: 10.1161/circresaha.116.304521

8. Greene HL. Sudden arrhythmic cardiac death—mechanisms, resuscitation and classification: the Seattle perspective. *Am J Cardiol*. 1990;65:4b–12b. doi: 10.1016/0002-9149(90)91285-e

9. Frantz S, Hundertmark MJ, Schulz-Menger J, Bengel FM, Bauersachs J. Left ventricular remodelling post-myocardial infarction: pathophysiology, imaging, and novel therapies. *Eur Heart J*. 2022;43:2549–2561. doi: 10.1093/eurheartj/ehac223

10. Tomaselli GF, Zipes DP. What causes sudden death in heart failure? *Circ Res*. 2004;95:754–763. doi: 10.1161/01.RES.0000145047.14691.db

11. Armbruster AL, Campbell KB, Kahanda MG, Cuculich PS. The role of inflammation in the pathogenesis and treatment of arrhythmias. *Pharmacotherapy*. 2022;42:250–262. doi: 10.1002/phar.2663

12. Herring N, Kalla M, Paterson DJ. The autonomic nervous system and cardiac arrhythmias: current concepts and emerging therapies. *Nat Rev Cardiol*. 2019;16:707–726. doi: 10.1038/s41569-019-0221-2

13. Ajijola OA, Lux RL, Khahera A, Kwon O, Aliotta E, Ennis DB, Fishbein MC, Ardell JL, Shivkumar K. Sympathetic modulation of electrical activation in normal and infarcted myocardium: implications for arrhythmogenesis. *Am J Physiol Heart Circ Physiol*. 2017;312:H608–h621. doi: 10.1152/ajpheart.00575.2016

14. Shen MJ, Zipes DP. Role of the autonomic nervous system in modulating cardiac arrhythmias. *Circ Res*. 2014;114:1004–1021. doi: 10.1161/circresaha.113.302549

15. Gardner RT, Ripplinger CM, Myles RC, Habecker BA. Molecular mechanisms of sympathetic remodeling and arrhythmias. *Circ Arrhythm Electrophysiol*. 2016;9:e001359. doi: 10.1161/circep.115.001359

16. Cao JM, Fishbein MC, Han JB, Lai WW, Lai AC, Wu TJ, Czer L, Wolf PL, Denton TA, Shintaku IP, et al. Relationship between regional cardiac hyperinnervation and ventricular arrhythmia. *Circulation*. 2000;101:1960–1969. doi: 10.1161/01.cir.101.16.1960

17. Fukuda K, Kanazawa H, Aizawa Y, Ardell JL, Shivkumar K. Cardiac innervation and sudden cardiac death. *Circ Res*. 2015;116:2005–2019. doi: 10.1161/circresaha.116.304679

18. Rubart M, Zipes DP. Mechanisms of sudden cardiac death. *J Clin Invest*. 2005;115:2305–2315. doi: 10.1172/jci26381

19. Zhou S, Chen LS, Miyauchi Y, Miyauchi M, Kar S, Kangavari S, Fishbein MC, Sharifi B, Chen PS. Mechanisms of cardiac nerve sprouting after myocardial infarction in dogs. *Circ Res*. 2004;95:76–83. doi: 10.1161/01.RES.0000133678.22968.e3

20. Hu H, Xuan Y, Xue M, Cheng W, Wang Y, Li X, Yin J, Li X, Yang N, Shi Y, et al. Semaphorin 3A attenuates cardiac autonomic disorders and reduces inducible ventricular arrhythmias in rats with experimental myocardial infarction. *BMC Cardiovasc Disord*. 2016;16:16. doi: 10.1186/s12872-016-0192-8

21. Li CY, Li YG. Cardiac sympathetic nerve sprouting and susceptibility to ventricular arrhythmias after myocardial infarction. *Cardiol Res Pract*. 2015;2015:698368. doi: 10.1155/2015/698368

22. Zhou S, Jung BC, Tan AY, Trang VQ, Gholmieh G, Han SW, Lin SF, Fishbein MC, Chen PS, Chen LS. Spontaneous stellate ganglion nerve activity and ventricular arrhythmia in a canine model of sudden death. *Heart Rhythm*. 2008;5:131–139. doi: 10.1016/j.hrthm.2007.09.007

23. Jiang H, Lu Z, Yu Y, Zhao D, Yang B, Huang C. Relationship between sympathetic nerve sprouting and repolarization dispersion at periinfarct zone after myocardial infarction. *Auton Neurosci*. 2007;134:18–25. doi: 10.1016/j.autneu.2007.01.014

24. Cao JM, Chen LS, KenKnight BH, Ohara T, Lee MH, Tsai J, Lai WW, Karagueuzian HS, Wolf PL, Fishbein MC, et al. Nerve sprouting and sudden cardiac death. *Circ Res*. 2000;86:816–821. doi: 10.1161/01.res.86.7.816

25. Rizas KD, Nieminen T, Barthel P, Zurn CS, Kahonen M, Viik J, Lehtimaki T, Nikus K, Eick C; Greiner TO, et al. Sympathetic activity-associated periodic repolarization dynamics predict mortality following myocardial infarction. *J Clin Invest*. 2014;124:1770–1780. doi: 10.1172/jci70085

26. Rizas KD, McNitt S, Hamm W, Massberg S, Kääb S, Zareba W, Couderc JP, Bauer A. Prediction of sudden and non-sudden cardiac death in post-infarction patients with reduced left ventricular ejection fraction by periodic repolarization dynamics: MADIT-II substudy. *Eur Heart J*. 2017;38:2110–2118. doi: 10.1093/eurheartj/ehx161

27. Rizas KD, Doller AJ, Hamm W, Vdovin N, von Stuelpnagel L, Zuern CS, Bauer A. Periodic repolarization dynamics as a risk predictor after myocardial infarction: prospective validation study. *Heart Rhythm*. 2019;16:1223–1231. doi: 10.1016/j.hrthm.2019.02.024

28. Bauer A, Klemm M, Rizas KD, Hamm W, von Stülpnagel L, Dommasch M, Steger A, Lubinski A, Flevari P, Harden M, et al. Prediction of mortality benefit based on periodic repolarisation dynamics in patients undergoing prophylactic implantation of a defibrillator: a prospective, controlled, multicentre cohort study. *Lancet*. 2019;394:1344–1351. doi: 10.1016/s0140-6736(19)31996-8

29. Boas R, Sappler N, von Stülpnagel L, Klemm M, Dixen U, Thune JJ, Pehrson S, Køber L, Nielsen JC, Videbæk L, et al. Periodic repolarization dynamics identifies ICD responders in nonischemic cardiomyopathy: a DANISH substudy. *Circulation*. 2022;145:754–764. doi: 10.1161/circulationaha.121.056464

30. Hamm W, Kassem S, von Stülpnagel L, Maier F, Klemm M, Schüttler D, Grabher F, Weckbach LT, Huber BC, Bauer A, et al. Deceleration capacity and periodic repolarization dynamics as predictors of acute mountain sickness. *High Alt Med Biol*. 2020;21:417–422. doi: 10.1089/ham.2020.0131

31. Schüttler D, Rudi WS, Bauer A, Hamm W, Brunner S. Impact of energy drink versus coffee consumption on periodic repolarization dynamics:

32. Schüttler D, von Stülpnagel L, Rizas KD, Bauer A, Brunner S, Hamm W. Effect of hyperventilation on periodic repolarization dynamics. *Front Physiol*. 2020;11:542183. doi: 10.3389/fphys.2020.542183

an interventional study. *Eur J Nutr*. 2022;61:2847–2851. doi: 10.1007/s00394-022-02853-8

33. Ebert TJ, Muzi M. Propofol and autonomic reflex function in humans. *Anesth Analg*. 1994;78:369–375. doi: 10.1213/00000539-199402000-00029

34. Clauss S, Schüttler D, Bleyer C, Vlcek J, Shakarami M, Tomsits P, Schneider S, Maderspacher F, Chataut K, Trebo A, et al. Characterization of a porcine model of atrial arrhythmogenicity in the context of ischaemic heart failure. *PLoS One*. 2020;15:e0232374. doi: 10.1371/journal.pone.0232374

35. Schüttler D, Tomsits P, Bleyer C, Vlcek J, Pauly V, Hesse N, Sinner M, Merkus D, Hamers J, Kääb S, et al. A practical guide to setting up pig models for cardiovascular catheterization, electrophysiological assessment and heart disease research. *Lab Anim (NY)*. 2022;51:46–67. doi: 10.1038/s41684-021-00909-6

36. Miyauchi Y, Zhou S, Okuyama Y, Miyauchi M, Hayashi H, Hamabe A, Fishbein MC, Mandel WJ, Chen LS, Chen PS, et al. Altered atrial electrical restitution and heterogeneous sympathetic hyperinnervation in hearts with chronic left ventricular myocardial infarction: implications for atrial fibrillation. *Circulation*. 2003;108:360–366. doi: 10.1161/01.Cir.0000080327.32573.7c

37. Oh Y-S, Jong AY, Kim DT, Li H, Wang C, Zemljic-Harpf A, Ross RS, Fishbein MC, Chen P-S, Chen LS. Spatial distribution of nerve sprouting after myocardial infarction in mice. *Heart Rhythm*. 2006;3:728–736. doi: 10.1016/j.hrthm.2006.02.005

38. Zhou S, Cao JM, Tebb ZD, Ohara T, Huang HL, Omichi C, Lee MH, Kenknight BH, Chen LS, Fishbein MC, et al. Modulation of QT interval by cardiac sympathetic nerve sprouting and the mechanisms of ventricular arrhythmia in a canine model of sudden cardiac death. *J Cardiovasc Electrophysiol*. 2001;12:1068–1073. doi: 10.1046/j.1540-8167.2001.01068.x

39. Zhao QY, Huang H, Zhang SD, Tang YH, Wang X, Zhang YG, Salim M, Okello E, Deng HP, Yu SB, et al. Atrial autonomic innervation remodelling and atrial fibrillation inducibility after epicardial ganglionic plexi ablation. *Europace*. 2010;12:805–810. doi: 10.1093/europace/euq089

40. Chang CM, Wu TJ, Zhou S, Doshi RN, Lee MH, Ohara T, Fishbein MC, Karagueuzian HS, Chen PS, Chen LS. Nerve sprouting and sympathetic hyperinnervation in a canine model of atrial fibrillation produced by prolonged right atrial pacing. *Circulation*. 2001;103:22–25. doi: 10.1161/01.cir.103.1.22

41. Ide C. Peripheral nerve regeneration. *Neurosci Res*. 1996;25:101–121. doi: 10.1016/0168-0102(96)01042-5

42. Meiri KF, Pfenninger KH, Willard MB. Growth-associated protein, GAP-43, a polypeptide that is induced when neurons extend axons, is a component of growth cones and corresponds to pp46, a major polypeptide of a subcellular fraction enriched in growth cones. *Proc Natl Acad Sci U S A*. 1986;83:3537–3541. doi: 10.1073/pnas.83.10.3537

43. Katritsis DG, Gersh BJ, Camm AJ. A clinical perspective on sudden cardiac death. *Arrhythmia Electrophysiol Rev*. 2016;5:177–182. doi: 10.15420/aer.2016.11:2

44. Clauss S, Bleyer C, Schuttler D, Tomsits P, Renner S, Klymiuk N, Wakili R, Massberg S, Wolf E, Kaab S. Animal models of arrhythmia: classic electrophysiology to genetically modified large animals. *Nat Rev Cardiol*. 2019;16:457–475. doi: 10.1038/s41569-019-0179-0

45. Schüttler D, Bapat A, Kääb S, Lee K, Tomsits P, Clauss S, Hucker WJ. Animal models of atrial fibrillation. *Circ Res*. 2020;127:91–110. doi: 10.1161/CIRCRESAHA.120.316366

46. Bharati S, Levine M, Huang SK, Handler B, Parr GV, Bauernfeind R, Lev M. The conduction system of the swine heart. *Chest*. 1991;100:207–212. doi: 10.1378/chest.100.1.207

47. Lelovas PP, Kostomitsopoulos NG, Xanthos TT. A comparative anatomic and physiologic overview of the porcine heart. *J Am Assoc Lab Anim Sci*. 2014;53:432–438.

48. Tranum-Jensen J, Wilde AA, Vermeulen JT, Janse MJ. Morphology of electrophysiologically identified junctions between Purkinje fibers and ventricular muscle in rabbit and pig hearts. *Circ Res*. 1991;69:429–437. doi: 10.1161/01.res.69.2.429

49. Santos-Gallego CG, Requena-Ibanez JA, San Antonio R, Ishikawa K, Watanabe S, Picatoste B, Flores E, Garcia-Ropero A, Sanz J, Hajjar RJ, et al. Empagliflozin ameliorates adverse left ventricular remodeling in nondiabetic heart failure by enhancing myocardial energetics. *J Am Coll Cardiol*. 2019;73:1931–1944. doi: 10.1016/j.jacc.2019.01.056

50. Daubner SC, Le T, Wang S. Tyrosine hydroxylase and regulation of dopamine synthesis. *Arch Biochem Biophys*. 2011;508:1–12. doi: 10.1016/j.abb.2010.12.017

51. Li W, Knowlton D, Van Winkle DM, Habecker BA. Infarction alters both the distribution and noradrenergic properties of cardiac sympathetic neurons. *Am J Physiol Heart Circ Physiol*. 2004;286:H2229–H2236. doi: 10.1152/ajpheart.00768.2003

52. Minardo JD, Tuli MM, Mock BH, Weiner RE, Pride HP, Wellman HN, Zipes DP. Scintigraphic and electrophysiological evidence of canine myocardial sympathetic denervation and reinnervation produced by myocardial infarction or phenol application. *Circulation*. 1988;78:1008–1019. doi: 10.1161/01.cir.78.4.1008

53. Simula S, Lakka T, Kuikka J, Laitinen T, Remes J, Kettunen R, Hartikainen J. Cardiac adrenergic innervation within the first 3 months after acute myocardial infarction. *Clin Physiol*. 2000;20:366–373. doi: 10.1046/j.1365-2281.2000.00278.x

54. Ajijola OA, Yagishita D, Patel KJ, Vaseghi M, Zhou W, Yamakawa K, So E, Lux RL, Mahajan A, Shivkumar K. Focal myocardial infarction induces global remodeling of cardiac sympathetic innervation: neural remodeling in a spatial context. *Am J Physiol Heart Circ Physiol*. 2013;305:H1031–H1040. doi: 10.1152/ajpheart.00434.2013

55. Wang Y, Suo F, Liu J, Hu H, Xue M, Cheng W, Xuan Y, Yan S. Myocardial infarction induces sympathetic hyperinnervation via a nuclear factor-κB-dependent pathway in rabbit hearts. *Neurosci Lett*. 2013;535:128–133. doi: 10.1016/j.neulet.2012.12.059

56. Yu TS, Wang X, Zhang HD, Bai RF, Zhao R, Guan DW. Evaluation of specific neural marker GAP-43 and TH combined with Masson-trichrome staining for forensic autopsy cases with old myocardial infarction. *Int J Leg Med*. 2018;132:187–195. doi: 10.1007/s00414-017-1590-x

57. Hartikainen J, Kuikka J, Mäntysaari M, Länsimies E, Pyörälä K. Sympathetic reinnervation after acute myocardial infarction. *Am J Cardiol*. 1996;77:5–9. doi: 10.1016/s0002-9149(97)89125-4

58. Campenot RB. Local control of neurite development by nerve growth factor. *Proc Natl Acad Sci U S A*. 1977;74:4516–4519. doi: 10.1073/pnas.74.10.4516

59. Perrone-Bizzozero NI, Neve RL, Irwin N, Lewis S, Fischer I, Benowitz LI. Post-transcriptional regulation of GAP-43 rnRNA levels during neuronal differentiation and nerve regeneration. *Mol Cell Neurosci*. 1991;2:402–409. doi: 10.1016/1044-7431(91)90027-l

60. Hassankhani A, Steinhelper ME, Soonpaa MH, Katz EB, Taylor DA, Andrade-Rozental A, Factor SM, Steinberg JJ, Field LJ, Federoff HJ. Overexpression of NGF within the heart of transgenic mice causes hyperinnervation, cardiac enlargement, and hyperplasia of ectopic cells. *Dev Biol*. 1995;169:309–321. doi: 10.1006/dbio.1995.1146

61. Chen P-S, Chen LS, Cao J-M, Sharifi B, Karagueuzian HS, Fishbein MC. Sympathetic nerve sprouting, electrical remodeling and the mechanisms of sudden cardiac death. *Cardiovasc Res*. 2001;50:409–416. doi: 10.1016/S0008-6363(00)00308-4

62. Hu H, Xuan Y, Wang Y, Xue M, Suo F, Li X, Cheng W, Li X, Yin J, Liu J, et al. Targeted NGF siRNA delivery attenuates sympathetic nerve sprouting and deteriorates cardiac dysfunction in rats with myocardial infarction. *PloS One*. 2014;9:e95106. doi: 10.1371/journal.pone.0095106

63. Solomon SD, Zelenkofske S, McMurray JJ, Finn PV, Velazquez E, Ertl G, Harsanyi A, Rouleau JL, Maggioni A, Kober L, et al. Sudden death in patients with myocardial infarction and left ventricular dysfunction, heart failure, or both. *N Engl J Med*. 2005;352:2581–2588. doi: 10.1056/NEJMoa043938

64. Adnet F, Renault R, Jabre P, Kulstad E, Galinski M, Lapostolle F. Incidence of acute myocardial infarction resulting in sudden death outside the hospital. *Emerg Med J*. 2011;28:884–886. doi: 10.1136/emj.2010.095885

65. O'Neill L. Estimating out-of-hospital mortality due to myocardial infarction. *Health Care Manag Sci*. 2003;6:147–154. doi: 10.1023/a:1024463418429

66. Maier B, Loewe A, Larscheid P, Behrens S, Bruch L, Busse R, Schaefer H, Schoeller R, Schühlen H, Theres H, et al. Out-of-hospital and in-hospital death from myocardial infarction in Berlin. *Gesundheitswesen*. 2021;83:291–296. doi: 10.1055/a-1152-4662

67. Akselrod S, Gordon D, Ubel FA, Shannon DC, Berger AC, Cohen RJ. Power spectrum analysis of heart rate fluctuation: a quantitative probe of beat-to-beat cardiovascular control. *Science*. 1981;213:220–222. doi: 10.1126/science.6166045

68. Malliani A, Pagani M, Lombardi F, Cerutti S. Cardiovascular neural regulation explored in the frequency domain. *Circulation*. 1991;84:482–492. doi: 10.1161/01.cir.84.2.482

69. Furlan R, Porta A, Costa F, Tank J, Baker L, Schiavi R, Robertson D, Malliani A, Mosqueda-Garcia R. Oscillatory patterns in sympathetic neural discharge and cardiovascular variables during orthostatic stimulus. *Circulation*. 2000;101:886–892. doi: 10.1161/01.cir.101.8.886

70. Rosenbaum DS, Albrecht P, Cohen RJ. Predicting sudden cardiac death from T wave alternans of the surface electrocardiogram: promise and pitfalls. *J Cardiovasc Electrophysiol*. 1996;7:1095–1111. doi: 10.1111/j.1540-8167.1996.tb00487.x

71. Nearing BD, Huang AH, Verrier RL. Dynamic tracking of cardiac vulnerability by complex demodulation of the T wave. *Science*. 1991;252:437–440. doi: 10.1126/science.2017682

72. Rosenbaum DS, Jackson LE, Smith JM, Garan H, Ruskin JN, Cohen RJ. Electrical alternans and vulnerability to ventricular arrhythmias. *N Engl J Med*. 1994;330:235–241. doi: 10.1056/nejm199401273300402

73. Shusterman V, Goldberg A, London B. Upsurge in T-wave alternans and nonalternating repolarization instability precedes spontaneous initiation of ventricular tachyarrhythmias in humans. *Circulation*. 2006;113:2880–2887. doi: 10.1161/circulationaha.105.607895

74. Hohnloser SH, Klingenheben T, Zabel M, Li YG, Albrecht P, Cohen RJ. T wave alternans during exercise and atrial pacing in humans. *J Cardiovasc Electrophysiol*. 1997;8:987–993. doi: 10.1111/j.1540-8167.1997.tb00621.x

75. McDonagh TA, Metra M, Adamo M, Gardner RS, Baumbach A, Böhm M, Burri H, Butler J, Čelutkienė J, Chioncel O, et al. 2021 ESC guidelines for the diagnosis and treatment of acute and chronic heart failure. *Eur Heart J*. 2021;42:3599–3726. doi: 10.1093/eurheartj/ehab368

76. Zeppenfeld K, Tfelt-Hansen J, de Riva M, Winkel BG, Behr ER, Blom NA, Charron P, Corrado D, Dagres N, de Chillou C, et al. 2022 ESC guidelines for the management of patients with ventricular arrhythmias and the prevention of sudden cardiac death. *Eur Heart J*. 2022;43:3997–4126. doi: 10.1093/eurheartj/ehac262

77. Al-Khatib SM, Stevenson WG, Ackerman MJ, Bryant WJ, Callans DJ, Curtis AB, Deal BJ, Dickfeld T, Field ME, Fonarow GC, et al. 2017 AHA/ACC/HRS guideline for management of patients with ventricular arrhythmias and the prevention of sudden cardiac death: a report of the American College of Cardiology/American Heart Association task force on clinical practice guidelines and the Heart Rhythm Society. *Circulation*. 2018;138:e272–e391. doi: 10.1161/cir.0000000000000549

78. Vaseghi M, Gima J, Kanaan C, Ajijola OA, Marmureanu A, Mahajan A, Shivkumar K. Cardiac sympathetic denervation in patients with refractory ventricular arrhythmias or electrical storm: intermediate and long-term follow-up. *Heart Rhythm*. 2014;11:360–366. doi: 10.1016/j.hrthm.2013.11.028

79. Meng L, Tseng CH, Shivkumar K, Ajijola O. Efficacy of stellate ganglion blockade in managing electrical storm: a systematic review. *JACC Clin Electrophysiol*. 2017;3:942–949. doi: 10.1016/j.jacep.2017.06.006

80. Hamm W, Vons L, Rizas KD, Vdovin N, Klemm M, Bauer A, Brunner S. Dynamic changes of cardiac repolarization instability during exercise testing. *Med Sci Sports Exerc*. 2019;51:1517–1522. doi: 10.1249/mss.0000000000001912

81. Sattler SM, Skibsbye L, Linz D, Lubberding AF, Tfelt-Hansen J, Jespersen T. Ventricular arrhythmias in first acute myocardial infarction: epidemiology, mechanisms, and interventions in large animal models. *Front Cardiovasc Med*. 2019;6:158. doi: 10.3389/fcvm.2019.00158

82. Chen WW, Xiong XQ, Chen Q, Li YH, Kang YM, Zhu GQ. Cardiac sympathetic afferent reflex and its implications for sympathetic activation in chronic heart failure and hypertension. *Acta Physiol (Oxf)*. 2015;213:778–794. doi: 10.1111/apha.12447

83. Jiang Z, Zhao Y, Doytchinova A, Kamp NJ, Tsai WC, Yuan Y, Adams D, Wagner D, Shen C, Chen LS, et al. Using skin sympathetic nerve activity to estimate stellate ganglion nerve activity in dogs. *Heart Rhythm*. 2015;12:1324–1332. doi: 10.1016/j.hrthm.2015.02.012